

TECHNICAL UNIVERSITY OF MOLDOVA

Department of Physics



As a manuscript

CZU: 05.45.-a, 42.65.Sf, 42.55.Px

GRIGORIEV EUGENIU

**PROPERTIES OF MULTI-SECTION SEMICONDUCTOR LASERS UNDER
EXTERNAL OPTICAL FEEDBACK**

131.03 – STATISTICAL AND KINETIC PHYSICS

Summary of the PhD thesis in physical sciences

CHISINAU, 2025

**This thesis was elaborated at the Department of Physics,
Doctoral School of the Technical University of Moldova**

Doctoral Committee:

MACOVEI Mihai, Doctor habilitate of Physical and Mathematical Sciences, Associate Professor, Institute of Applied Physics, State University of Moldova, **President of the Doctoral Commission.**

SANDULEAC Ionel, Doctor of Physical Sciences, Associate Professor, Technical University of Moldova, **Secretary of the Doctoral Commission.**

TRONCIU Vasile, Doctor habilitate of Physical and Mathematical Sciences, Professor, Technical University of Moldova, **Supervisor of postgraduate student, Member.**

BARDETCHE Profir, Doctor of Physical and Mathematical Sciences, Associate Professor Institute of Applied Physics, State University of Moldova, **Member the Doctoral Commission.**

Official references:

NICA Denis, Doctor habilitate of Physical Sciences, Associate Professor, State University of Moldova.

OSTROVSKI Sergey, Doctor habilitate of Physical and Mathematical Sciences, Associate Professor, Institute of Applied Physics, State University of Moldova.

URSACHI Veaceslav, Corresponding Member of ASM, Doctor habilitate of Physical and Mathematical Sciences, Associate Professor, Academy of Sciences of Moldova.

The thesis defense will take place on 27 March 2025, at 13:00 in the meeting of the Doctoral Commission within the Doctoral School of the Technical University of Moldova (approved by the decision of the Scientific Council of 3 July 2024, minutes no. 5), Bd. Ștefan cel Mare 168, Study Block no. 1 of TUM, room 1-205, Chișinău, MD - 2004, Republic of Moldova.

The doctoral thesis and the scientific summary can be consulted at the Technical and Scientific Library of the Technical University of Moldova and on the ANACEC website ("<http://anacec.md/>").

The abstract was sent on 21 February 2025.

Scientific Secretary of the Doctoral Commission,

PhD in Physical Sciences, Associate Professor



SANDULEAC Ionel

Scientific leader

PhD in Physics and Mathematics, University Professor



TRONCIU Vasile

Author



GRIGORIEV Eugeniu

© Grigoriev Eugeniu, 2025

CONTENTS

CONCEPTUAL GUIDELINES OF RESEARCH	3
THESIS CONTENT	9
GENERAL CONCLUSIONS AND RECOMMENDATIONS	28
BIBLIOGRAPHY	30
Annex 1. List of publications on the topic of the thesis	31
ANNOTATION	34
SUMMARY	34

CONCEPTUAL GUIDELINES OF RESEARCH

Actuality of the topic and the importance of the problem investigated. Semiconductor lasers with quantum dot and well active media represent an innovative class of optoelectronic devices that use multi-section structures, offering significant advantages in efficiency and performance, a narrower emission spectrum and improved thermal stability compared to traditional lasers. Their main feature is the ability to obtain more precise light emissions with a narrower spectrum and improved efficiency, essential for various applications, from optical communications to quantum technologies. With all these advantages, the development and implementation of semiconductor lasers involves complex technologies for growing multi-section structures, minimizing energy losses and advancing to impurity-free structures. Semiconductor lasers are already used in fields such as biophysics, medicine, spectroscopy, etc. We would like to mention that the development and fabrication of these lasers involves advanced crystal growth and semiconductor device fabrication techniques. Controlling the dimensions of the active medium components, either wells or quantum dots, is essential for achieving the laser performance required for the above-mentioned applications. Continued development in this area promises to bring new innovations and applications in the future of laser technology and optoelectronics.

A problem currently faced by the field of semiconductor lasers is the variability and reproducibility in laser fabrication, energy losses through non-radiative processes, such as non-radiative recombination processes, which can affect the efficiency and performance of lasers, degradation and thermal stability. It is worth mentioning that multi-section lasers, being sensitive to temperature fluctuations in some sections, can affect their performance. Thus, the cost-effective integration of new laser products into existing optoelectronic technologies is an important subject of study for practical applications.

We would like to mention some promising directions for semiconductor lasers such as the development of quantum technologies, such as quantum computers and quantum cryptography, by improving photonic control and manipulation at the quantum level, high-speed optical communications, which provide high-capacity data transfer, medical and biotechnological applications through biomedical imaging and non-invasive treatments. Last but not least, semiconductor lasers can be integrated into high-precision optical sensors for detecting and measuring a diverse range of parameters, such as temperature, pressure in gases and chemicals, etc. Research in this field not only brings innovation, but also has a significant impact on fundamental research.

Description of the situation in the research field and identification of research problems.

The situation in the field of theoretical research on semiconductor lasers is dynamic and attracts significant interest from the scientific and industrial community, due to their potential to revolutionize optoelectronic technology. Aspects such as improving the efficiency and performance of lasers, optimizing manufacturing processes and integrating these devices into existing systems are under discussion in various national and international research centers. A crucial aspect in semiconductor laser research is the use of new semiconductor materials that offer improved performance. These efforts require a deep understanding of the quantum phenomena that occur in multi-section layers and active media, either wells or quantum dots, and an integrated approach that combines expertise in physics, engineering and chemistry. Research in the field of semiconductor lasers has recently focused on the development of new semiconductor materials with improved optoelectronic properties for their use in laser production. Optimization of the dimensions and composition of the active medium to obtain light emissions leads to the emergence of devices with specific characteristics. This may involve the use of advanced fabrication techniques to control the thickness, length and chemical composition of the active medium. Another major concern is improving the efficiency and stability of laser emission. At the time of formulating the research problem of this thesis, various problems were identified that existed in explaining the experimental results in the research field. Some phenomena could not be explained by existing theoretical models. Thus, it was necessary to develop new models that could explain the experimental results. Last but not least, the exploration of new applications and technologies such as high-speed optical communications, high-precision optical sensors, medical imaging and quantum technologies have boosted theoretical research. Finally, we mention that the use of advanced numerical simulations helps to evaluate structures with high-performance characteristics that are subsequently realized in experiments. Cooperation between experimentalists, theorists and partnerships with industry lead to the identification of the potential of new and emerging applications of semiconductor lasers. In recent decades, semiconductor lasers have shown wide scientific interest because they have been widely used in various experiments of new phenomena in physics, as well as phenomena in nonlinear dynamics.

In conclusion, the current situation in the field of semiconductor laser research is a dynamic one, in which remarkable advances are accompanied by significant technological challenges.

The purpose of the thesis consists of the theoretical study of the stationary and dynamic behavior of semiconductor lasers with multiple sections and optical feedback, the proposal of new devices with different topologies, the analysis of bifurcations and scenarios leading to the appearance of instabilities and the proposal of ways to avoid them, the development of

computational programs for performing numerical simulations, the theoretical explanation of the phenomena observed in experiments, the establishment of the areas of use of new laser structures in optical communication, spectroscopy, quantum metrology, medicine, etc.

Research objectives:

1. Adjusting the theoretical model of the semiconductor laser with quantum dot active medium to the action of an optical feedback coming from an external Fabry Perot resonator. Obtaining the stationary states of the laser in the case of the presence of an air layer between the resonator and the active medium. Plotting the distributions of the external cavity modes in the plane of different parameters. Establishing the optimal operating conditions of the laser in the continuous wave regime;
2. Development of a theoretical model of the behavior of lasers with distributed Bragg reflectors (DBR) that allow operation in a single longitudinal mode with a narrow spectral linewidth. Theoretical study of the dynamic properties of a laser with a built-in DBR section that is under the influence of external optical feedback. Proposal of a model with the main parameters dependent on the wavelength of the primary mode. Identification of the nature of the bifurcations that occur in such a system. Tracing regions with instabilities in the plane of different material and geometric parameters of the laser;
3. Study of the behavior of high-power devices with narrow spectral band emission and spatially limited diffraction, the so-called monolithic integrated master oscillator power amplifiers (MOPA). Determination of the mechanism of the influence of the pumping from the PA section on the MO section by thermal heating. Theoretical investigation of the experimentally observed emission collapse of the MOPA device. Quantitative explanation of the available experimental results, in particular, the power collapse in the case of current injection into a control section adjacent to the distributed Bragg reflector laser. Comparison of theoretical results with experimental ones;
4. Analysis of the dynamics of different types of lasers that generate self-pulsations and short-duration pulse trains. Determination of the parameters and the mode of influence of the blue light laser parameters, such as the influence of the thickness of the saturation absorber, the laser length, as well as the lifetime of the charge carriers on self-pulsations. Theoretical study of the DFB laser structure for generating self-pulsations and short-duration pulses. Determination of the mechanism of generating short-duration pulses;
5. Numerical modeling by simulating nonlinear dynamic effects of semiconductor lasers with active medium wells and quantum dots.

Scientific research methodology. The theoretical support for the thesis was accumulated following the analysis of the specialized literature in the field of semiconductor laser theory. To successfully achieve the above objectives, the following theoretical methods and models were applied:

1. Bifurcation analysis methods were used to determine the bifurcations that occur in the studied systems;
2. The DDE-biftool software and computational methods, such as the Runge-Kutta method of degree IV, were used;
3. Numerical calculations of the Bloch model adapted with the theoretical part were performed for the optical feedback coming from the Fabry-Perot resonator with an air layer between the active medium and the resonator;
4. Numerical calculations were performed for the adapted model in which for the first time the main parameters are wavelength dependent and the results compared with those obtained in the Lang-Kobayashi model;
5. The traveling wave model was used to study the dynamics of high-power MOPA lasers;
6. The rate model was proposed for generating short pulses in an excitable DFB laser;
7. Programs were developed in Matlab, Fortran and C++ for numerical simulations in the case of direct integration of differential equations with delay.

Scientific novelty and originality of research.

The scientific novelty of the results obtained consists of:

1. The theoretical model for the structure of the double-feedback quantum dot laser with air section between the resonators has been extended. The extended model allows obtaining the distribution of stationary states, i.e., of the external cavity modes in the plane of different parameters;
2. A new model of DBR reflector lasers operating in a single longitudinal mode with a narrow spectral linewidth has been developed. This model takes into account the main laser parameters dependent on the wavelength of the primary mode and is consistent with experimental results. The case of the laser under the influence of external optical feedback has been analyzed;
3. The mechanism of the influence of the pumping from the PA amplification section on the MO master oscillator section was theoretically established. This influence was achieved by thermal heating of a multi-section MOPA device. The experimentally observed emission collapse of the MOPA device was theoretically confirmed and explained. The quantitative theoretical results are consistent with the available experimental data;

4. The mechanism for generating short-duration pulses of a DFB laser was determined;
5. High-frequency self-pulsations have been obtained in InGaN lasers with a saturable absorber;
6. Numerical simulations of the nonlinear dynamic effects of multi-cavity semiconductor lasers with external optical feedback were performed.

The scientific problem solved is: proposals for the realization of new laser structures with multiple sections and controllable properties. The theoretical results obtained in the thesis were explained and compared with the experimental ones provided by colleagues from Humboldt University, Berlin, "Germany". As a result of numerical simulations, the appropriate parameters for the optimal operation of laser systems with multiple sections for use in various fields such as spectroscopy, optical communication, quantum metrology, medicine, etc. were obtained.

The theoretical significance and applicative value of the work consists of:

- Theoretical treatment of the structure of the quantum dot laser with double feedback and air section between the resonators. Determination of the distribution of stationary states, i.e. of the external cavity modes in the plane of different parameters, which proved to be much more complex than in the case of conventional feedback;
- Theoretical development of a model of the DFB laser with optical feedback having the main laser parameters dependent on the wavelength of the primary mode;
- Identification of the mechanism of the influence of the pumping from the PA amplification section on the MO section of the MOPA multi-section laser by thermal heating. Theoretical confirmation of the emission collapse of the MOPA device observed in the experiment;
- Proposing new laser devices for generating self-pulsations and short-duration pulses.

The practical value of the thesis lies in explaining various phenomena reported in the specialized literature, some of them obtained in the experimental research of our colleagues at Humboldt University.

- estimation of material and geometric parameters of multi-section lasers to improve external emission control;
- practical recommendations for configuring lasers with controllable properties in different applications;
- implementing the results obtained in the thesis in two scientific projects.

Main scientific results submitted for defense:

1. The external cavity mode distribution of the double feedback quantum dot laser was obtained which is completely different from that of conventional feedback, and the proposed laser structure is compact and can be easily integrated with existing optical communication systems;
2. A new model has been proposed that adequately describes the behavior of air-cavity DBR lasers subjected to strong external feedback. The idea of this model lies in the dependence of laser parameters on wavelength. It has been shown that model parameters such as the Henry factor, photon lifetime, feedback strength and modal group index strongly depend on the mismatch between the laser wavelength and the Bragg wavelength. Stable stationary states pass into unstable ones through Hopf bifurcations. It has been shown that DBR lasers with short active sections are characterized by unstable regions. The theoretical explanation of the instabilities lies in the existence of a wide instability region for large values of the Henry factor in these regions;
3. The complex behavior of the monolithic multi-section DBR MOPA system was explained using the traveling wave model. The presence of the laser emission collapse observed in the experiments was theoretically demonstrated, which is caused by the thermal detuning of both laser sections. It was shown that for a stable operation of the MOPA device a front facet reflectivity of less than 10^{-4} is required. Numerical simulations are in good agreement with the available experimental results;
4. It was observed that pulse generation can be done by an excitable DFB laser with a built-in passive dispersive reflector. In particular, short-duration pulses with a symmetrical shape were obtained.

Approval of the results obtained.

The main scientific results were presented at the following conferences and seminars:

1. The 6th International Conference on Nanotechnologies and Biomedical Engineering, ICNBME-2023, September 20-23, 2023, Chisinau, Republic of Moldova.
2. The seventh edition of the International Colloquium 'Physics of Materials' - PM-7, University POLITEHNICA of Bucharest, in collaboration with The Romanian Academy of Scientists on November 10-11, 2022, Bucharest, Romania.
3. The 5th International Conference on Nanotechnologies and Biomedical Engineering ICNBME-2021, November 3-5, 2021, Chisinau, Republic of Moldova.

4. Technical and scientific conference of students, master's and doctoral students. March 29, 2022. Chisinau, Republic of Moldova.
5. Technical and scientific conference of students, master's and doctoral students. March 23-25, 2021. Chisinau, Republic of Moldova.
6. Conference on Electronics, Communications and Computing: IC|ECCO-2021, Ed. 11, October 21-22, 2021, Chisinau, Republic of Moldova.
7. Technical and scientific conference of students, master's and doctoral students, April 1-3, 2020, Chisinau, Republic of Moldova.
8. Seminars of the Laser Devices and Nanostructured Materials Research Laboratory, Department of Physics, UTM.

Publications on the topic of the thesis.

The main results of the thesis were published in 16 scientific papers, of which 4 articles in international journals ranked ISI and SCOPUS, 3 in journals from the National Register of specialized journals category B+, 5 articles in proceedings of national conferences with international participation, 4 theses at scientific forums, international conferences. The list of the author's contributions to the thesis topic is presented at the end of the summary in Appendix 1.

Thesis volume and structure of thesis.

The thesis consists of an introduction, five chapters, general conclusions and recommendations. The thesis is presented on 137 pages, with 3 tables and 64 figures. The bibliography contains 136 references. The thesis was developed within the Research Laboratory of Laser Devices and Nanostructured Materials, Department of Physics, Technical University of Moldova with participation in the project under State Programs 20.80009.5007.08 entitled “Study of optoelectronic structures and thermoelectric devices with high efficiency” and in the project 15.817.02.22F “Thermoelectric and optical properties of nanostructured materials and quantum dot devices”.

THESIS CONTENT

Introduction describes the relevance of the thesis topic, as well as the purpose, objectives and scientific novelty of the research.

Chapter I is a review of the theory of semiconductor lasers, as well as the properties of lasers with different topologies for different applications [1]. The semiconductor laser is described as a cost-effective and reliable alternative to gas lasers. The advantages of semiconductor lasers such as small size, low manufacturing costs, wide use, long lifespan, etc. are mentioned. Details related to the practical realization of semiconductor lasers are described by studying the material

composition and dimensionality [2]-[6] on obtaining the gain. The fundamental theory, concept and properties of semiconductor lasers are exposed. Semiconductor lasers are described as a recent development in the field of laser technology. The properties of DFB lasers are defined [7]-[9] and the complicated phenomena that occur in them are described. Also, different methods of controlling laser emission are described. At the end of this Chapter, recently published results in the field of MOPA devices have been described [10].

In Chapter 2 results of the study of the stationary states of the laser with quantum dots as active medium with optical feedback are presented. The behavior of the laser with quantum dots as active medium with feedback from an external Fabry-Perot resonator was studied. The complex model of the Bloch equations was used, in which the photon annihilation rate and polarization decay have a similar order of magnitude. The parameters used in numerical calculations were obtained for later use in the creation of new laser devices. The initial equations were normalized so that in the end equations for dimensionless quantities were obtained. The dimensionless equations represent a system of nonlinear differential equations with delay describing the dynamics of the quantum dot laser with optical feedback considered in this chapter. The solutions of the system of differential equations with delay were analyzed in the form of the so-called external cavity modes. Following some mathematical transformations, a transcendental equation for the frequency of the external cavity modes was obtained at first. Later, the amplitude values of the laser field intensity and the polarization vector were obtained. Finally, the charge carrier density was determined, which is the solution of the third-order equation. The graphs were drawn of the external cavity mode (ECM) distributions in the two-parameter plane. The shape of the mode distribution is complicated when the feedback strength in the second branch increases, thus the “bell” shape and the deformed satellite ellipses are present. Thus, we found that, for a high feedback strength, the shape of the external mode location becomes more complex. The results of this Chapter were presented in the papers [A2], [A4], [A7], [A10], [A13] in Appendix no. 1.

The schematic model of the quantum dot laser is shown in Fig. 1.

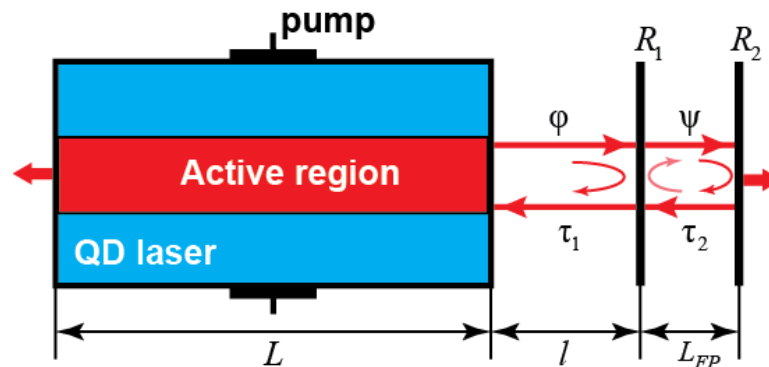


Fig.1.Schematic view of the quantum dot laser.

This laser consists of the layer representing the active medium with GaN quantum dots and an external Fabry-Perot resonator. We consider the structure shown in Fig. 1 and the model of the laser with quantum dot active medium, using the following system of Bloch equations [11], [12] in which E is the field amplitude, p is polarization, N is the inversion, and the terms Γ_1 and Γ_2 describe double feedback

$$\frac{dE}{dt} = -\kappa E + 2Z^{OD}\Gamma|g|p + \frac{Z^{OD}\Gamma\beta F_P}{\tau_{sp}E^*} \left(\frac{N+1}{2}\right)^2 + \Gamma_1 e^{i\varphi} E(t-\tau_1) + \Gamma_2 e^{i\psi} E(t-\tau_2), \quad (1)$$

$$\frac{dp}{dt} = -\gamma p + |g|EN, \quad (2)$$

$$\frac{dN}{dt} = -4|g|Ep + \frac{N_0(w_e) - N}{T_1(w_e)} - \frac{F_P}{\tau_{sp}} \left(\frac{N+1}{2}\right)^2. \quad (3)$$

The number of quantum dots in the active region of the laser is denoted by Z^{OD} . $t_1 = 2l/c$ and $t_2 = 2L_{FP}/c_g$ are the delay times between the laser and the resonator and in the resonator, respectively.

We analyze the solutions of the system of equations (1)-(3) in the form of the so-called ECMs

$$E = E_s e^{i\omega_s t}; \quad p = p_s e^{i\omega_s t + i\alpha_s}; \quad N = N_s. \quad (4)$$

Using (4) from (1)-(3) for the frequency of the external cavity modes, the following transcendental equation is obtained for ω_s :

$$\omega_s = -\Gamma_1 \sin(\omega_s \tau_1 + \varphi) - \Gamma_2 \sin(\omega_s \tau_2 + \psi), \quad (5)$$

and the amplitude values of the laser field intensity and the polarization vector:

$$E_s = \sqrt{\frac{1}{CN_s} \left[\frac{d_0 - N_s}{\tilde{T}_1} - \frac{1}{\tilde{\tau}_{eff}} \left(\frac{N_s + 1}{2}\right)^2 \right]}, \quad p_s = \sqrt{\frac{\tilde{g}^2 N_s}{C\tilde{\gamma}^2} \left[\frac{d_0 - N_s}{\tilde{T}_1} - \frac{1}{\tilde{\tau}_{eff}} \left(\frac{N_s + 1}{2}\right)^2 \right]}. \quad (6)$$

Charge carrier density N_s is the solution of the third-order equation

$$\tilde{T}_1 D N_s^3 + \left[\tilde{T}_1 \Gamma_f + 2\tilde{T}_1 D - 4\tau_{eff} A \right] N_s^2 + \left[T_1 D + 2\Gamma_f (T_1 + 2\tau_{eff}) + 4d_0 A \tau_{eff} \right] N_s + \Gamma_f (T_1 - 4d_0 \tau_{eff}) = 0. \quad (7)$$

Distributions of the external cavity modes in the plane $(N_s - \omega_s)$ is shown in Fig. 2. It can be seen that the modes are not located on the ellipse, but on a "bell" shape.

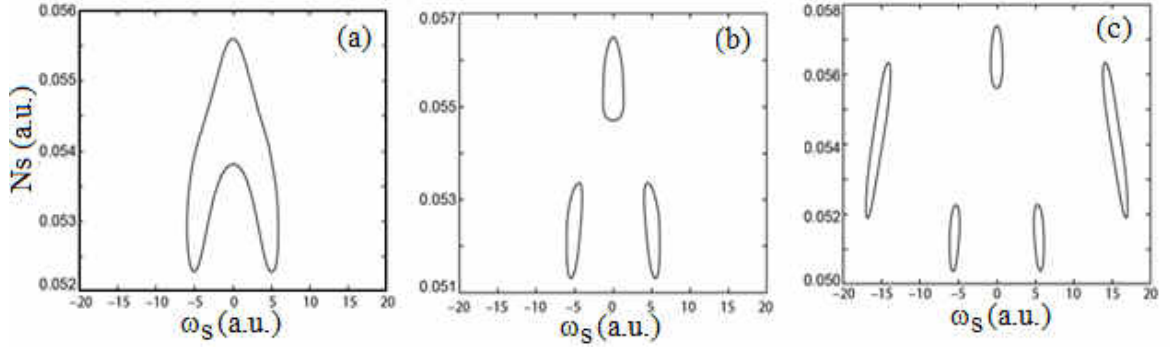


Fig. 2. Distribution of ECMs in the two-parameter plane ($N_s - \omega_s$) for (a) $\Gamma_1 = 5, \Gamma_2 = 5$, (b) $\Gamma_1 = 5, \Gamma_2 = 10$, (c) $\Gamma_1 = 5, \Gamma_2 = 15$. $\tau_1 = 0.2$, $\tau_2 = 0.5$.

Figure 3 shows the ECMs distribution for higher feedback power in the first branch of the external cavity $\Gamma_1 = 15$ and a small feedback power in the second $\Gamma_2 = 5$. A more complicated distribution of ECM can be observed in contrast to conventional feedback.

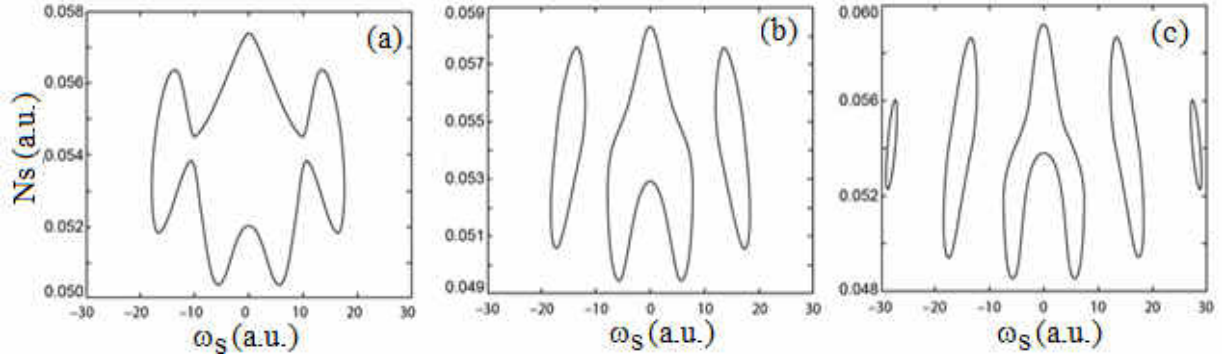


Fig. 3. Distribution of ECMs in the two-parameter plane ($N_s - \omega_s$) for (a) $\Gamma_1 = 15, \Gamma_2 = 5$, (b) $\Gamma_1 = 15, \Gamma_2 = 10$, (c) $\Gamma_1 = 15, \Gamma_2 = 15$. $\tau_1 = 0.2$, $\tau_2 = 0.5$.

Thus, we mention that in this Chapter the steady states of the quantum dot active medium laser under the influence of optical feedback were obtained. We demonstrated that the ECMs are located in the "bell" shape for a low feedback power. Higher feedback intensities imply the appearance of deformed satellite ellipses.

In Chapter 3 the theory of DBR lasers was developed. These lasers allow operation in the regime of a single longitudinal mode with a small spectral linewidth. The dynamic properties of a laser with a built-in DBR section, which is under the influence of external optical feedback, were theoretically studied. The Lang-Kobayashi model was used to verify the results of the model proposed in this chapter for small reflection coefficients. The model used in this chapter is completely different from the one used for Fabry–Perot lasers, since the main parameters depend on the wavelength of the primary mode, i.e., on the reduction of the effectiveness of the primary laser mode. The nature of the bifurcations that occur in such a system was identified. The

bifurcations that occur in the laser plus feedback system were plotted. The Hopf bifurcation was determined and plotted in the plane of various parameters. It was shown that this bifurcation is responsible for the instabilities that occur in such a laser. The necessary conditions for the stable operation of the laser in the continuous wave regime were identified. It was also demonstrated the influence of the active region length on the stability of the device emission and it was shown how this property is modified by varying the laser mode mismatch from the solitary one. The results presented in this Chapter provide a good basis for more detailed experimental studies of DBR lasers and their applications as a stable single-mode light source. The results of this chapter were published in the papers [A3], [A16] in Appendix no. 1.

Figure 4 shows the schematic of the DBR laser studied in this Chapter. The laser emission from the front facet is transmitted by a wavefront and reflected by a distant mirror with reflectivity R . The phase shifts of the mirrors and the external mirror facets have been taken into account. φ is the phase of the external mirror, τ is the external feedback delay. The wavelength of the primary laser λ_λ is $1.12 \mu\text{m}$. The optical losses in the DBR section are 200 m^{-1} . The central wavelength λ_κ of the laser DBR is $1.12 \mu\text{m}$. The reflectivity of the front face of the active region is $R_a = 0.1$.

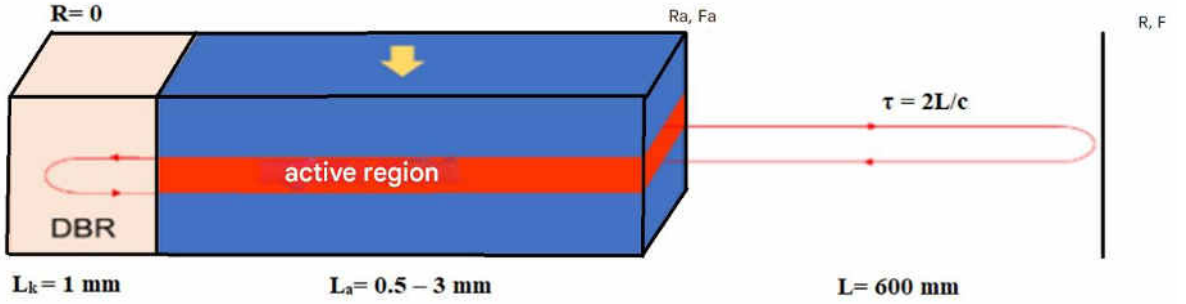


Fig. 4. Schematic of the DBR laser with external optical feedback.

Under continuous wave (CW) operating conditions, the charge carrier densities as well as the optical power in the DBR laser are constant over time. Two counter-propagating waves of the following form circulate throughout the laser:

$$E(z, t) = \left[E^+(z, t, \omega_s) e^{-i\beta_0 z} + E^-(z, t, \omega_s) e^{i\beta_0 z} \right] e^{i\omega_s t}, \quad (8)$$

where $\beta_0 = n\pi / \Lambda$ with order n and network period Λ in the DBR.

The scaled feedback power is obtained using \tilde{q} from [13] with the following form:

$$\eta = \frac{\sqrt{R/R_a}}{|\partial_{\omega_s} \tilde{q}|}, \quad \text{with} \quad q(\omega_s, g_s) = \frac{1 - \rho(\omega_s, g_s)}{R_a - \rho(\omega_s, g_s)}. \quad (9)$$

The phase is written in the form:

$$\phi = \varphi + \arg(\partial_{\omega_s} \tilde{q}) - \frac{\pi}{2} - \arg(r). \quad (10)$$

The Henry factor can be written as:

$$\tilde{\alpha}_H = -\frac{\text{Re}(\partial_g \tilde{q} / \partial_{\omega} \tilde{q})}{\text{Im}(\partial_g \tilde{q} / \partial_{\omega} \tilde{q})}. \quad (11)$$

The scaled photon lifetime has the form:

$$\tilde{\tau}_p = (\tilde{v}_g g_l)^{-1}, \quad \text{with} \quad \tilde{v}_g = +2 \text{Im}(\partial_g \tilde{q} / \partial_{\omega} \tilde{q}). \quad (12)$$

The threshold conditions are given by the following expression:

$$g_l = \alpha_a - \frac{1}{L_a} \ln(|r_k(\omega_l)| \sqrt{R_a}). \quad (13)$$

We construct the reflectivity that enters (12), that is, the reflectivity on the right side of a lattice is [14]

$$r_k = \frac{-ik \frac{+\sin(\gamma L_k)}{\gamma}}{\cos(\gamma L_k) + i\beta \frac{\sin(\gamma L_k)}{\gamma}} \quad \text{with} \quad \gamma = \sqrt{(\Delta\beta_k)^2 - k^+ k^-}, \quad (14)$$

where L_k , is the lattice length, and the wavelength mismatch $\Delta\beta_k(\lambda)$ is:

$$\Delta\beta_k(\lambda) = \beta_k(\lambda) - \beta_0, \quad \beta_k = \frac{2\pi}{\lambda} n_k(\lambda) - \frac{i}{2} \alpha_k, \quad k^\pm = k e^{\mp 2\pi i \varphi_k}. \quad (15)$$

Here k is the coupling coefficient of the grating, n_k is the modal index of the internal waveguide, α_k is the background absorption coefficient of the guided waves in the grating section, φ_k is a phase shift depending on the relative position of the grating with respect to the right facet of the DBR. The stationary states are given by rotating wave solutions, i.e. ECMs $E = E_s e^{i\omega_s t}$. Using these solutions we obtain a transcendental equation for ω_s :

$$i\omega_s = i\omega_1 + (1 + i\tilde{\alpha}_H) \frac{N_s}{\tilde{\tau}_p} + \eta e^{-(\phi + \tau\omega_s)}. \quad (16)$$

The real part of this equation represents the charge carrier density:

$$\frac{N_s}{\tilde{\tau}_p} = -\eta \cos(\tau\omega_s + \phi), \quad (17)$$

and from the imaginary part we obtain a transcendental equation:

$$\omega_s - \omega_1 = -\eta \left[\tilde{\alpha}_H \cos(\tau\omega_s + \phi) + \sin(\tau\omega_s + \phi) \right]. \quad (18)$$

In Fig. 5 we present a demonstration of the validity of our model compared to the Lang – Kobayashi one, the dependence of the standing mode amplification on the wavelength of the standing mode for the LK model (black line) and the model proposed in this Chapter - red line, as well as the results obtained using the DDE-biftool software program. For the reflectivity

$R = 10^{-4}$ of the mirror, a good agreement between the models is observed, through very good overlap of the ellipses.

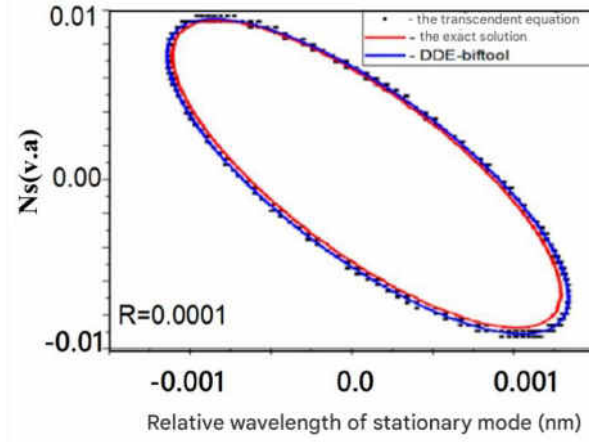


Fig. 5. LK model versus full model for different feedback reflectivity $R = 10^{-4}$. Length of the active section $L_a = 1.0$ mm.

An important issue is investigating the stability of stationary states. Here we use the DDE-biftool software for delay differential equations [15] to analyze the stability of the external cavity modes based on a parameter continuation method. Figure 6 shows the ellipse of the external cavity modes for $R = 10^{-4}$ and the active section length $L_a = 1.0$ mm.

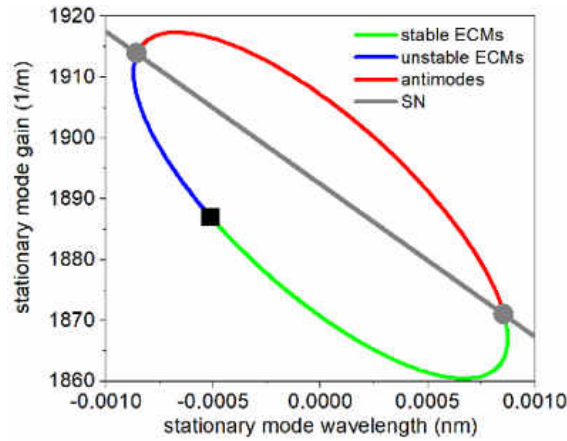


Fig. 6. External cavity mode curve for active section length $L_a = 1.0$ mm ($I_{tr} = 0.013$ A, $I_{th} = 0.0262$ A and $I = 0.0524$ A) and external facet reflectivity $R = 10^{-4}$. The solid green line corresponds to the stable steady state, and the blue line – to the unstable steady state. Gray circle - node-saddle bifurcation for $R = 10^{-4}$. The node-saddle bifurcation depicted by the gray line is for any reflectivity. Square – Hopf bifurcation.

The gray lines constitute a saddle-node (SN) bifurcation for any value of the external mirror reflectivity R . The intersection points between this line and the ellipses shown by gray circles

represent SN bifurcations for $R = 10^{-4}$, separating ECMs called “anti-modes” (red lines) from the modes. The solid red line in this figure is not of interest for our investigations. DDE-biftool allows the identification of Hopf bifurcations marked with a black square in Fig. 6, separating stable (green line) and unstable (blue line) ECMs.

Figure 7 shows the Hopf lines separating the stable and unstable regions in terms of two device parameters, namely the external reflectivity R and the external phase. φ .

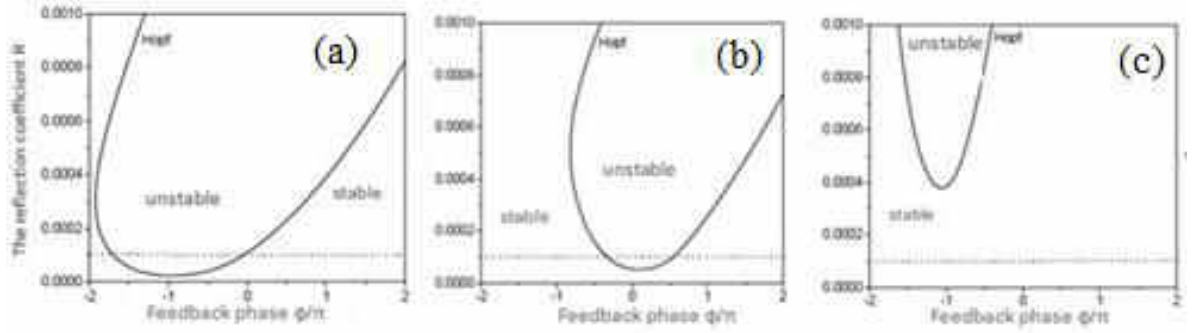


Fig. 7. Hopf bifurcation in the two-parameter plane (external reflectivity R - external phase φ/π). (a) $L_a = 0.5$ mm, (b) $L_a = 1.0$ mm (c) $L_a = 3.0$ mm.

We mention that the other Hopf lines obtained by a repetition, with a period of 2π are not displayed. This figure confirms the results of previous findings and also those obtained in [16], where a semi-analytical model was used. Thus, for the laser with $L_a = 0.5$ mm the instability region is very wide (Fig. 7(a)). An increase in the cavity length of the active region leads to a narrowing of the unstable regions and a wider stable region (Fig. 7(b)). We observe that further increase in the cavity length reduces the unstable region (Fig. 7(c)).

Thus, in this Chapter we propose results of theoretical investigations of the behavior of a DBR laser subjected to external feedback. The case of a long feedback branch was considered. A full model and an adapted Lang-Kobayashi model were used to calculate the steady states. Good agreement was obtained between the model proposed in this Chapter and the LK model for external reflectivities lower than 10^{-4} .

In Chapter 4 was studied the behavior of high-power devices with narrow-band spectral emission and spatially limited diffraction MOPA. We would like to mention that the MO section is realized either as a waveguide DFB laser or as a DBR laser. It was shown that pumping in the PA section can perturb the MO section by thermal heating or optical feedback, resulting in the appearance of spatiotemporal instabilities, such as self-pulsations, longitudinal multimode operation and a deterioration of the spatial beam properties. Thus, in this Chapter, it was proposed to decouple the MO and PA sections. Between them, an additional section with a separate electrical contact, called a preamplifier or control section (CON), can be introduced. The introduction of the

new CON section makes the system more complex. It was experimentally found that the introduction of such a section can lead to a collapse of the laser emission. Thus, in this Chapter, the origin of the mentioned phenomenon was theoretically investigated. The study was started for the MOPA laser emitting at 1064 nm, using the traveling wave equation (TWE) model in which the coupling of the propagating fields in both directions is taken into account. The numerical model used in this chapter quantitatively explains, in particular the available experimental results, the power collapse in the case where the current is injected into a control section adjacent to the distributed Bragg reflector laser. The influence of the reflection index of the back face of the MOPA on the laser behavior was also investigated.

The multi-section MOPA laser studied in this Chapter and schematically shown in Fig. 8, is similar to the device reported in [17]. The only difference is that we replaced the conical PA amplification section in [17] with a linear one. Such a simplification allows for a correct qualitative description [18]. The DBR MOPA laser consists of 5 sections, namely (in Fig. 8 from right to left): a 1 mm long DBR section joined by a 0.75 mm long G amplification section, a 0.25 mm long DBR section, a 0.5 mm long preamplifier or control section and a 3.5 mm long PA amplification section. The total length of the device is 6 mm. The active layer with three InGaAs quantum wells extends over all sections. Both sides of the device are coated with an anti-reflection coating. For numerical simulations, we set the reflection coefficient of the back facet (DBR2) to zero and vary the reflection coefficient of the front facet of the PA amplifier from 0 to 10^{-2} .

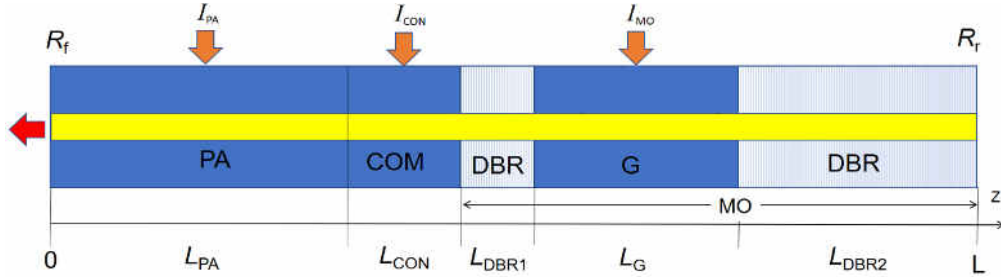


Fig. 8. Schematic view of the DBR MOPA device showing the lengths of the sections and the currents in them.

The numerical model used is based on the 1×1 time \times axial position traveling wave equations, for the slowly varying complex amplitudes $E^+(z, t)$ and $E^-(z, t)$ of the counter propagating optical fields in each section of the device.

$$\frac{n_g}{c_0} \frac{\partial}{\partial t} E^\pm = \left[\pm \frac{\partial}{\partial z} - i\Delta\beta(N, I) \right] E^\pm - ikE^\pm + F_{sp}^\pm. \quad (19)$$

For each individual amplitude $E^+(z, t)$ and $E^-(z, t)$ we can write:

$$\frac{n_g}{c_0} \partial_t E^+ + \partial_z E^+ = -i\beta E^+ - ikE^- + F_{sp}^+, \quad (20)$$

$$\frac{n_g}{c_0} \partial_t E^- - \partial_z E^- = -i\beta E^- - ikE^+ + F_{sp}^-, \quad (21)$$

where c_0 is the speed of light in vacuum, F_{sp}^\pm is the stochastic contribution of spontaneous emission, n_g the group index and k the field coupling coefficient due to the Bragg grating. The relative propagation factor in each section is given by the relationship:

$$\Delta\beta = \delta_0 - i\frac{\alpha_0}{2} + k_0 [\Delta n_N(N) + \Delta n_T(I)] + i\frac{g(N) - D}{2}, \quad (22)$$

where δ_0 is the static mismatch between the sections, which is due to different refractive indices of the modes, α_0 gives internal optical losses, $k_0 = 2\pi/\lambda_0$ where λ_0 is the reference wavelength. D is the linear operator that models the dispersion of the gain. It is assumed that the modal gain depends logarithmically on the charge carrier density:

$$g(N) = \Gamma g' N_r \ln\left(\frac{N}{N_r}\right), \quad (23)$$

where Γ is the optical confinement factor, g' the differential amplification coefficient and N_r charge carrier density at transparency. The dependence of the variation of the modal index on the charge carrier density is given by the function:

$$\Delta n_N = \tilde{\alpha}_H \frac{\Gamma g' N_r}{k_0} \sqrt{\frac{N}{N_r}}. \quad (24)$$

function $\Delta n_T(I)$ from (22) describes the change in modal index in a laser section k due to self- and cross-heating induced by the currents injected into the section r

$$\Delta n_{T,k} = \frac{n_g}{\lambda_0} \sum C_k^r \cdot I_r, r, k \in [PA, CON, DBR1, G, DBR2], \quad (25)$$

being the major factor that involves transitions between longitudinal modes when the injection current is varied. We note that in our calculations we only consider the changes in the modal indices induced by the currents injected into adjacent sections, incorporated in LDSL [18]. Figure 9(a) depicts the dependence of the optical output power of the signal at the front facet of the PA section on the current injected into the G amplification section of the MO. The threshold current is 100 mA, similar to that obtained in the experiment (see Fig. 9(c)). When the current of the amplification section of the MO part is increased, the output power also increases with a typical saw tooth shape caused by the jumps of the longitudinal modes. The period of the mode jumps is $\Delta I_{MO} \approx 53$ mA, a feature similar to that observed in the experiment (Fig. 9(c)). We note that for

high injection current intensities we obtain values of hundreds of mW of the output signal power. Figure 9b shows an optical mapping of the spectral density for the variation of the injected current in the G region. The almost periodic jumps from a mode with a longer wavelength to a mode with a shorter wavelength is observed ($\Delta\lambda_{MOD} \approx 0,134$ nm). In addition to the mode hopping, there is also a variation in the overall laser wavelength, which is mainly determined by the peak reflectivity of the DBR sections. Immediately after the threshold current, the overall wavelength decreases due to the optical generation of charge carriers in the DBR section, resulting in a decrease in the modal index. For higher currents, the heating of the DBR sections (given by the DBR parameters) $C_{DBR1}^G = C_{DBR2}^G$ dominates, resulting in a shift of the length towards larger values. In a time interval between mode jumps, the wavelength of the modal field increases with the increase in the current determined by C_G^G . For $I_{MO} = 0.3$ A, the slope of the curve is $\delta\lambda_{MOD}/\delta I = 2,1$ nm/A and the slope of the total wavelength shift is $\delta\lambda_{OVE}/\delta I = 0,25$ nm/A. These values, as well as the distance between the longitudinal modes (given $\Delta\lambda_{MOD}$) are similar to those obtained in the experiment.

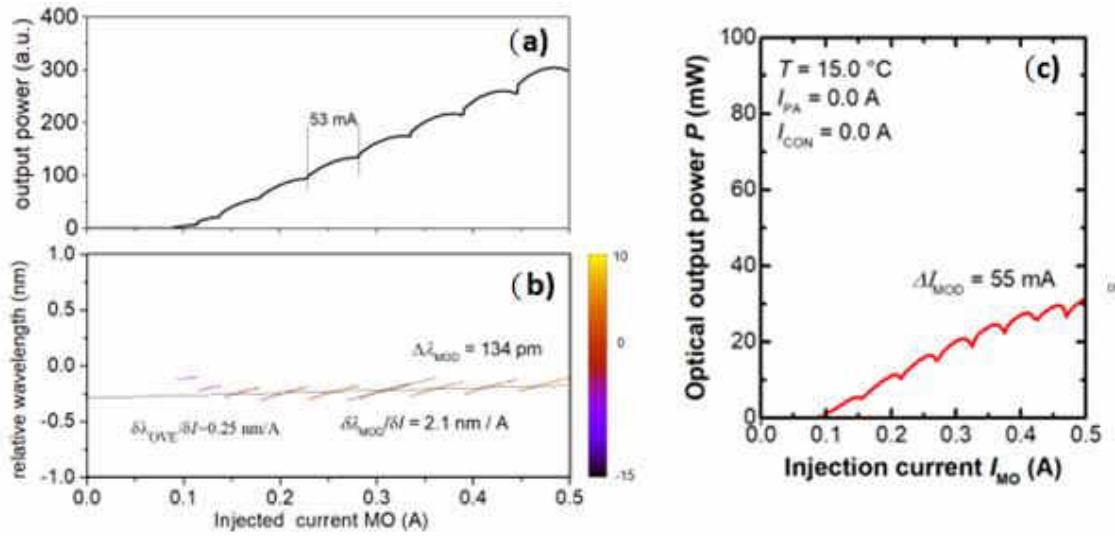


Fig. 9. a) Theory: laser signal output power calculated as a function of the current injected into the G amplification section of the MO part. b) Pseudo-color mapping of optical spectral densities (in dB) as a function of the current in the G region of the MO part. c) Experimental results - optical output power as a function of the current of the MO section. The current in the PA and CON sections is zero. The currents in the PA and CON sections are equal to zero. The reflectivity of the front facet is equal to zero.

The black line in Fig. 10(a) shows the dependence of the output signal power on the current intensity in the CON region for a current of the G region of the MO part fixed at 0.15 A. The

output power increases from 45 mW to a maximum value of 170 mW for an ICON current of 0.2 A and shows a bend at the value $I_{CON} \approx 110 \text{ mA}$. A further increase in the ICON current above 0.2 A leads to a sudden decrease in the emerging power and no laser emission is observed (laser collapse), a process similar to that observed in the experiment (Fig. 10(b)). For $I_{MO} = 0,3 \text{ A}$ a similar behavior is observed, but between I_{CON} currents of 0.3 A and 0.45 A laser emission occurs again (see blue line in Fig. 10(a)). The output power starts to increase from 160 mW at the injected current $I_{CON} = 0$ and reaches a maximum value of 460 mW for $I_{CON} = 0.44 \text{ A}$. For a current of the G section of the MO component part of 0.45 A the output power increases from 280 mW followed by jumps and nonlinearities up to a maximum power of 640 mW at an ICON current of 0.45 A (red line in Fig. 10(a)). The output power decreases to zero for I_{CON} of 0.5 A.

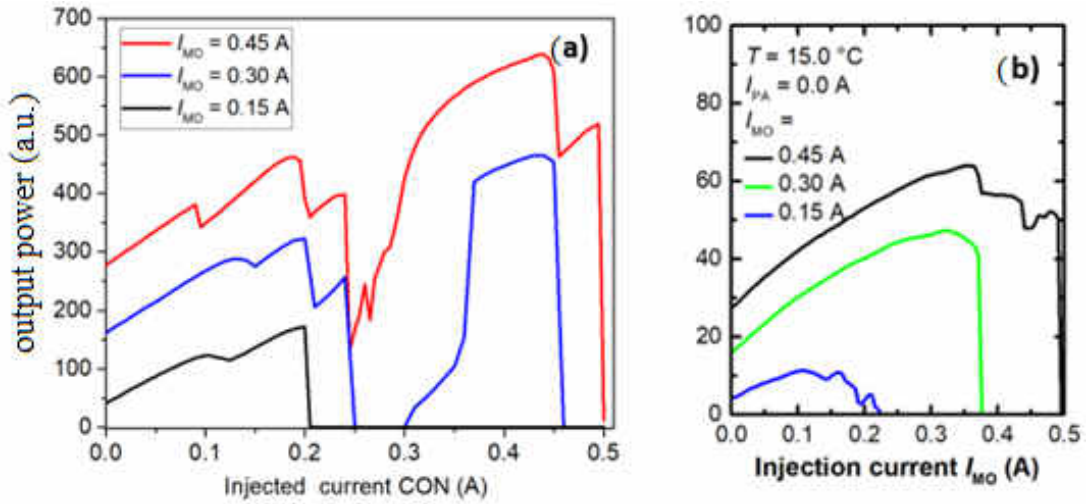


Fig. 10. a) Theory: the output power of the laser signal as a function of the current injected into the control section for different currents of the G section of the MO region. Experimental results: b) The optical output power as a function of the CON section current. The reflection coefficient of the front facet of the laser is equal to zero.

Next, a simplified version of the laser is proposed for a coincidence with the one used in another experiment of our colleagues in Berlin. Only the amplification section G has a length of 0.5 mm and is complemented by DBR sections of 1 mm and 0.5 mm in length on the left and right sides, respectively. The MO region is connected to the 4 mm power amplifier PA. The entire length of the device is 6 mm, and the emission wavelength is 1120 nm and differs from the one investigated above. Unlike the previous case, in this scheme the currents are injected into the MO region section and the power amplifier PA. We recall that in the previous case the current in the PA amplification region is kept at zero. The investigated structure was grown by epitaxy in the

metal-organic vapor phase. The active layer consists of an InGaAs double quantum well, asymmetrically embedded in a 4.8 μm thick vertical waveguide core.

The laser dynamics are analyzed using equations (18) – (24) with the values of the main laser parameters used in the numerical simulations collected in the Table below.

Table 1, Basic parameters of MOPA

Symbol	Description	unit	Value
λ_0	Reference wavelength	m	$1,12 \cdot 10^{-6}$
L_G	Active section length	m	$0,5 \cdot 10^{-3}$
L_{dbr1}	DBR 1 section length	m	$1,0 \cdot 10^{-3}$
L_{dbr2}	DBR 2 section length	m	$0,5 \cdot 10^{-3}$
I_{PA}	Length of PA section	m	$4,0 \cdot 10^{-3}$
R_r	Back facet intensity reflectivity		0
R_f	Front facet intensity reflectivity		$0 \dots 0,1$

In the following we will discuss the output characteristics of the device compared to the experimental ones. The experiment was done at room temperature. Figure 11 illustrates both the numerically calculated and the experimentally obtained output power as a function of the current injected into the PA amplification section for a fixed current of 200 mA injected into the MO region.

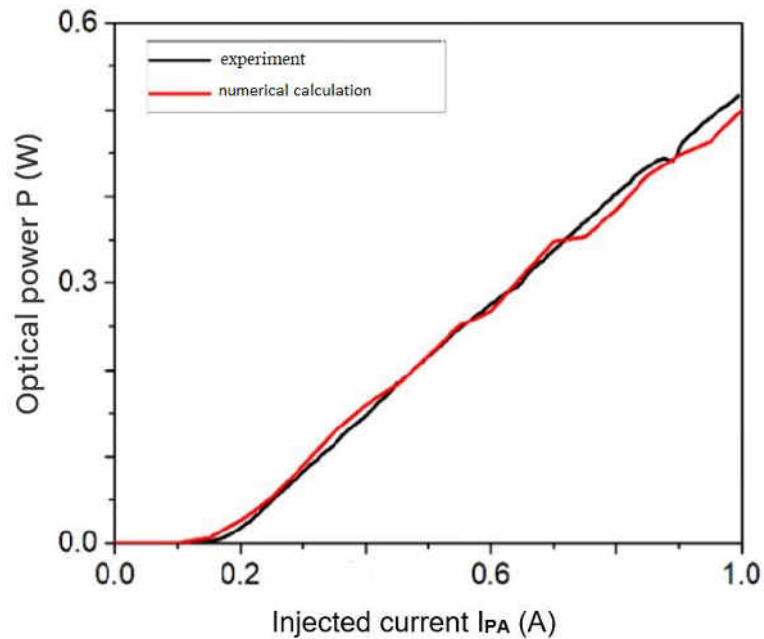


Fig. 11. Dependence of the output signal power from the laser on the current injected into the power amplifier PA: red – numerical calculations, black – experimental data. The current injected into the MO region is 200 mA. The reflection coefficient of the front facet is zero ($R = 0$).

From these characteristics, a threshold of 0.15 A and a slope of 0.6 W/A can be determined. This figure indicated a good agreement between the numerical calculations and the experimental results. Next, we examine the same dependence as in Figure 12, namely, what happens if the reflection coefficient of the front facet increases from zero to 10^{-2} . Figure 12a represents the power – injected current characteristics obtained in the experiment.

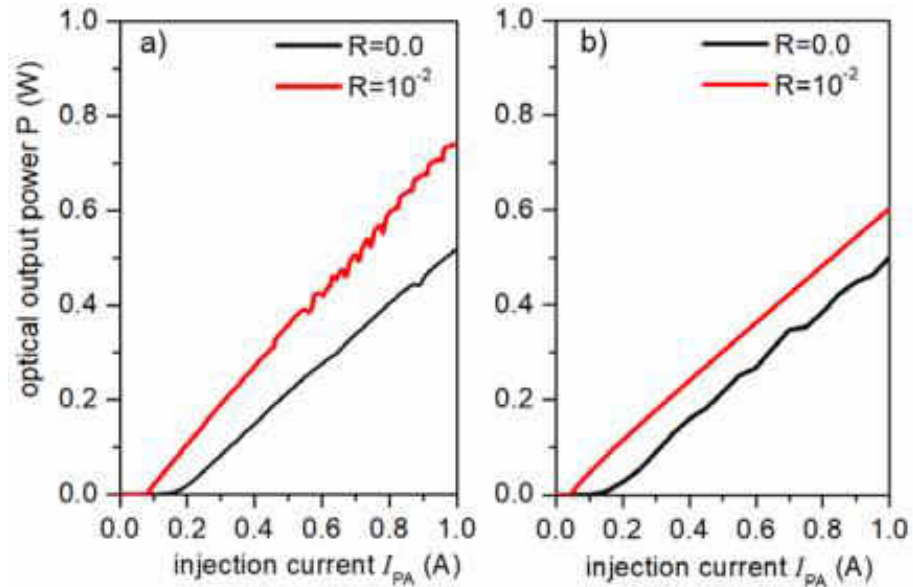


Fig. 12. Output power as a function of the injection current in the PA amplifier section for two values of the front face reflection coefficient. The injected current in the MO section is fixed at 200 mA: a) experiment, b) numerical calculations.

As mentioned earlier, for zero reflection coefficient, the threshold current is 0.16 A. On the other hand, an increase in the front facet reflectivity reduces the threshold current to 0.09 A (red curve in Figure 13(a)). An increase in the slope up to 0.78 W/A can be observed. This is due to the fact that, for a finite value of the front facet reflection coefficient, the system acts as a compound cavity. In addition, for high currents, ripples are observed in the dependence of the output power on the injected current. Typically, this ripple region is characterized by instabilities, which are not the subject of this research. Figure 13(b) represents the results obtained in the numerical calculation. We observe a good agreement between the experiment and the numerical calculations in terms of the decrease in the threshold current (0.05 A). The slope of the curve increases slightly (0.60 W/A). We note that both results indicate good agreement between numerical calculations and experimental results.

This Chapter presents the results of numerical investigations of the behavior of the monolithic DBR MOPA system with multiple sections. Two similar structures but emitting at different frequencies were theoretically studied. The traveling wave model adapted to MOPA devices with multiple sections was used. The characteristics observed in the experiment were reproduced and explained, as well as the dependence of the optical power of the pre-amplifier on the control current. The presence of laser emission collapse caused by a thermal mismatch of both DBR sections of the investigated structure was demonstrated. Numerical simulations show a transition between the operating modes of the MOPA system and a laser with multiple sections if the reflection coefficient of the front facet increases. For stable MOPA operation, a front facet reflectivity of 10^{-4} or less is required for the proper operation of the system. We mention that the theoretical results were compared with the experimental ones. A good agreement was obtained between the experimental data and the results of numerical simulations. The results of this Chapter were published in the papers [A1], [A6] and [A9] in Annex no. 1.

In Chapter 5 the dynamics of different types of lasers that generate self-pulsations and short-duration pulse trains are described. At the beginning of the Chapter, theoretical results of the influence of blue light laser parameters, such as the influence of the thickness of the saturation absorber, the laser length, and the lifetime of the charge carriers on self-pulsations were presented. The investigated laser consists of the InGaN active layer and a saturation absorber. Both the active layer and the saturation absorber are composed of 3 InGaN quantum wells. The Hopf bifurcation curve calculated for the self-pulsation region was plotted in the plane of the various parameters mentioned above. It was demonstrated that the range of resonator lengths 400 – 500 μm is the most favorable for generating self-pulsations with frequencies between 2 and 3 GHz. In the second part of this Chapter, another DFB laser structure for generating self-pulsations and short-duration pulses was theoretically investigated. The investigated structure of DFB lasers has an additional passive dispersive reflector. The active and passive sections are integrated together in a complex chip. The reflection between the sections is considered to be very small. The analysis of the dynamics of the DFB laser with a passive dispersive reflector was performed based on the rate equations. It was demonstrated that the generation of pulses in the case presented in this Chapter is related to the excitable properties of the laser. In the excitable regime, by injecting a small perturbation into the system, symmetrical pulses were obtained at the laser output (see [A2], [A5], [A8], [A11], [A13], [A14] in Appendix no. 1).

Figure 13 shows a configuration of the investigated laser consisting of an InGaN active layer and a saturation absorber. Both the active layer and the saturation absorber are composed of

3 InGaN quantum wells. The thickness of the active region and the saturation absorber is 18 nm, and the wavelength is 405 nm. The length of the active layer is 650 μm .

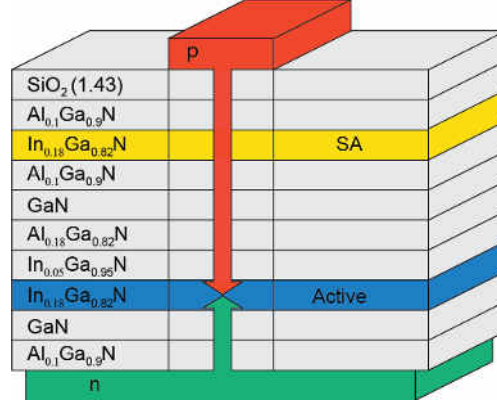


Fig. 13. Setup of InGaN laser.

The theoretical model used to describe the dynamics of the InGaN laser is based on the model proposed in [19],[20]

$$\frac{dS}{dt} = \left[\frac{\sum_i a_i \xi_i (N_i - N_{gi})}{V_i} - BS - G_{th} \right] S + \frac{M \sum_i a_i \xi_i N_i}{V_i} \quad (26)$$

$$\frac{dN_i}{dt} = -\frac{a_i \xi_i}{V_i} (N_i - N_{gi}) S - \frac{N_i}{\tau_{si}} + \sum_{j \neq i} \left(\frac{N_j}{T_{ij}} - \frac{N_i}{T_{ji}} + \frac{I_{ji} - I_{ij}}{e} \right) \quad (27)$$

where S is the number of photons, N_i - the number of charge carriers injected into region i , a_i - the differential amplification coefficient, ξ_i - the field limiting factor, N_{gi} is the number of charge carriers transferred through region i , τ_{si} represents the charge carrier lifetime and T_{ij} is the time duration equivalent to the charge carrier lifetime during their diffusion from region j to region i . I_{ji} is the charge carrier intensity injected from region j to region i . V_i - the volume of the laser sections determined by the expression $V_i = W_i d_i L$, where L is the laser length, and d_i and W_i are, respectively, the thickness and width of these sections.

Figure 14 shows the Hopf bifurcation curve (black line) calculated for the self-pulsation region in the differential gain plane as a function of the current injected into the active region. The red line in Figure 14 separates the boundary between the “off” and “on” laser operating regions.

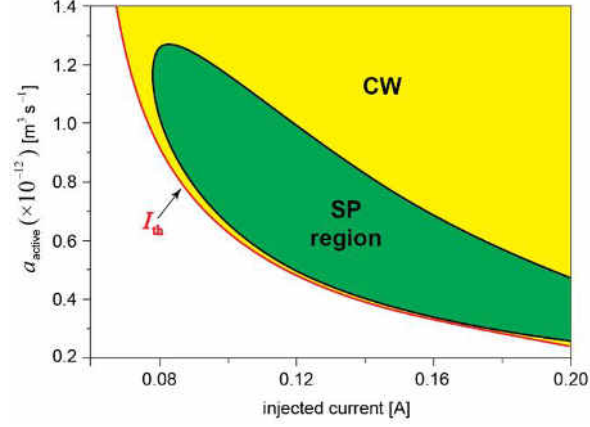


Fig. 14. Bifurcation diagram for a resonator length of 650 μm . The self-pulsation region in the differential gain plot as a function of the injected current (green region). The threshold value of the current is indicated by the red line. The black line indicates the Hopf bifurcation.

In Fig. 15, the self-pulsation regions are illustrated as a function of the laser resonator length on a) the differential amplification coefficient and b) the lifetime of the charge carriers in the absorber. These regions were obtained for the InGaN laser parameters and the current intensity fixed at 150 mA.

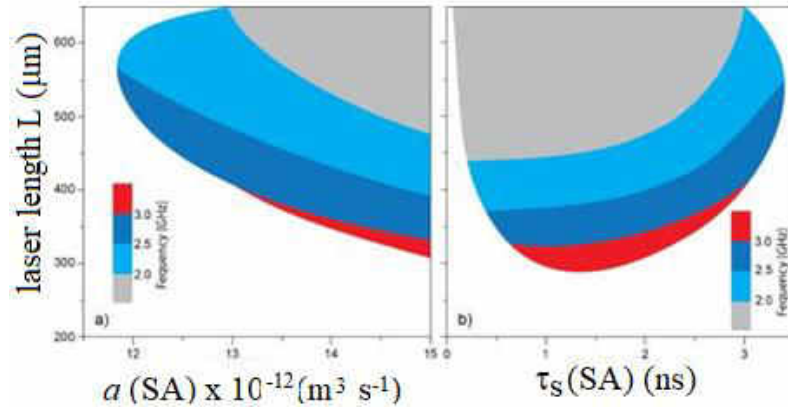


Fig. 15. Variation of the self-pulsation frequency in the plane: resonator length as a function of (a) α_{SA} the differential amplification coefficient in the absorber and (b) τ_{SA} the lifetime of the charge carriers in the absorber.

Next, we analyze another laser structure for generating self-pulsations and short-duration pulses. A sketch of the investigated structure of DFB lasers with an additional passive dispersive reflector is shown in Fig. 16. The pump current is applied to the active region. A small current for phase variation and control is also applied. The active and passive sections are integrated together in a complex chip. The reflection between the sections is assumed to be very small. It is well known that similar devices are used for generating high-frequency single-mode self-pulsations. A single-mode approximation was proposed in [21] and used to discuss the behavior of self-

pulsations and excitability [22]. Here we focus on the generation of pulses when the laser operates in the excitability regime.

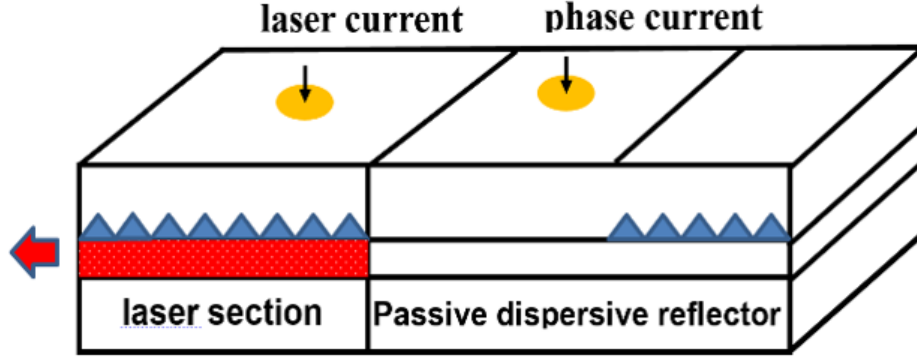


Fig. 16. DFB laser with additional passive dispersive reflector in longitudinal direction. The main injected current is applied to the active section. The control current is applied to the phase section for the variation of the mismatch n_0 .

We begin our analysis based on the rate equations [21]

$$\frac{dn}{dt} = J - n - (1 + n)K(n)P + n_{\text{perturb}}, \quad \frac{dP}{dt} = TG(n)P, \quad (28)$$

where n and P are the dimensionless carrier and photon number, respectively. τ is the dimensionless time. The parameter J is the relative excess injection rate ($1 < J < 10$). T is the ratio of the charge carrier to the photon lifetime. The functions $K(n)$ and $G(n)$ in equations (27) describe the influence of the reflector on the laser dynamics [21] approximated by:

$$K(n) = K_0 + \frac{AW^2}{4(n - n_0)^2 + W^2}, \quad G(n) = n_0 + \alpha \cdot \Delta n \cdot \tanh\left(\frac{n}{\Delta n}\right),$$

where A , W , K_0 , n_0 are constants. n_0 is the mismatch between the resonance peak of the function $K(n)$ and the threshold density $n = 0$. This mismatch can be controlled in real devices by adjusting the parameter T . The amplitude of the perturbation is above the threshold. From this figure we distinguish the nature of the phase current. Figure 17(a) shows the time evolution of the photon number for different slow-fast values of the system for small values of the parameter T . Thus, for $T = 100$, the output photon number P increases and then forms a long (slow) excursion in the phase space until returning to the stationary state (see Fig. 18(b) black line). For large values of the parameter T the long excursion in the phase plane disappears. For the reference, value of the parameter $T = 500$.

We note that in this case the pulse generated by the system is almost symmetrical and could be used in various applications as a short pulse generator.

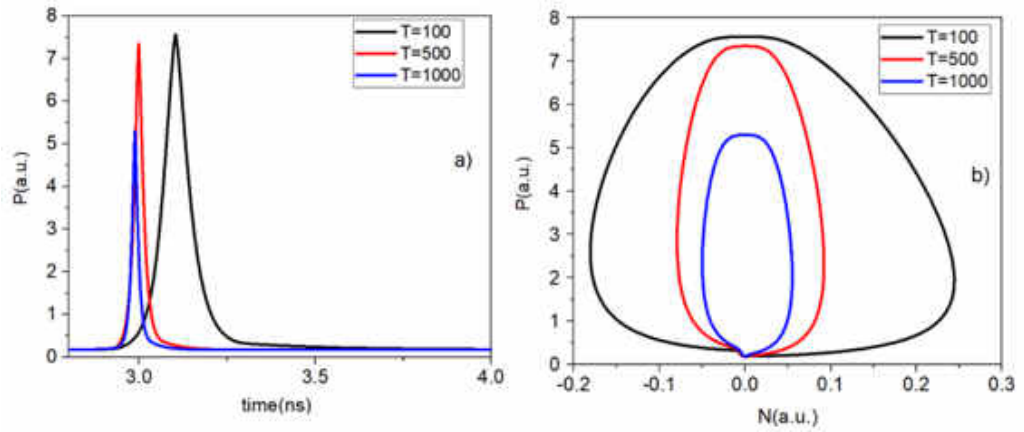


Fig. 17. (a) Time evolution of the number of photons P for different values of the parameter T . (b) phase portraits in the $(P - n)$ plane.

Figure 18(a) represents the dependence of the number of photons for the case when the perturbation is smaller than the threshold. As can be seen, the laser is in the “off” state with small oscillations around the equilibrium state. Figure 18(b) shows the pulse generation by the passive dispersive reflector laser under the influence of the train of perturbations with different amplitudes. The current pulses supplied with the pulse width of 0.05 ps have a delay time of 0.05 ps between them.

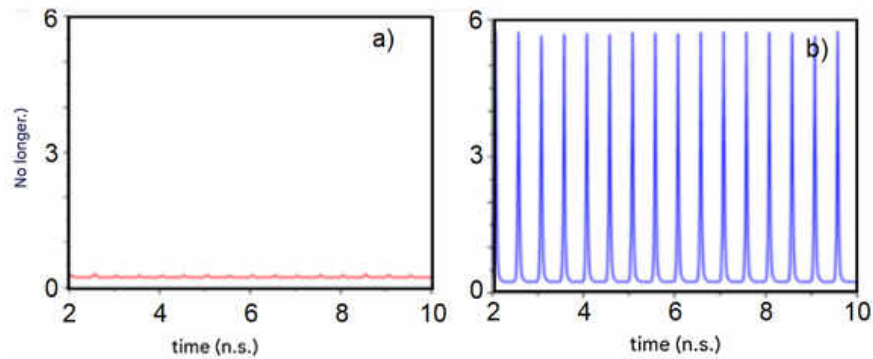


Fig. 18. Dependence of the number of photons P on time for different values of the applied perturbation: (a) laser in "off" state; (b) pulse generation.

This Chapter presents the results obtained from numerical calculations for lasers of different types that generate AP and short-duration pulses. The dynamics of blue light lasers with self-pulsations were investigated. The self-pulsation domains were obtained in the plane of the different laser parameters. Subsequently, the results of investigations on the generation of pulses by an excitable DFB laser with a built-in passive dispersive reflector were reported. It was found that for small perturbations no laser response is observed. On the other hand, when the perturbation is above the threshold, the periodic response was observed.

GENERAL CONCLUSIONS AND RECOMMENDATIONS

The importance of this thesis lies in the presentation of theoretical results, compared to the available experimental ones, of the nonlinear dynamics of semiconductor lasers with different topologies.

The general conclusions are as follows:

1. The Bloch equation model was used and adjusted for feedback from an external Fabry-Perot resonator with an air section between the laser and the resonator, the expressions for the amplitude values of the laser field intensity and the polarization vector were obtained, as well as a third-order algebraic equation for determining the charge carrier density, as well as a transcendental equation for determining the external cavity modes. The distribution of stationary states of the quantum dot active medium laser was obtained, which is completely different from that of conventional feedback. We found that the ECMs are located on the "bell" shape for low feedback power. Larger feedbacks imply the appearance of deformed satellite ellipses. (Chap.2, §2.2- §2.5).
2. The results of theoretical investigations of the behavior of a DBR laser subjected to external feedback are presented for the case of a long feedback branch. A concordance of the distribution of stationary states of the complete model proposed in this work, in which the parameters are wavelength dependent, is demonstrated versus the conventional Lang-Kobayashi model. This agreement between the models is valid for reflectivities as low as 10^{-3} . In the model proposed in this work, the adapted Henry factor, the photon lifetime, the feedback power and the modal group index entering the LK model depend strongly on the mismatch between the laser wavelength and the Bragg wavelength. Stable stationary states pass into unstable ones through Hopf bifurcations. We have shown that DBR lasers with short active sections are characterized by wider unstable regions compared to those of long ones. We attribute the existence of a wide instability region to the negative mismatch of the high Henry factor values characteristic of this region. A positive detuning implies a reduction of the unstable region (low alpha factor), even a disappearance for detuning between higher positive frequencies. We believe that the presented results provide a good basis for future studies and, in particular, provide some clues for more detailed experimental investigations of DBR lasers and their applications as a stable single-mode light source. (Chap.3, §3.2- §3.5).
3. The results of numerical investigations of the behavior of two monolithic multi-section MOPA DBR systems emitting at different frequencies were obtained using the adapted traveling wave model. It was possible to reproduce and explain the characteristics observed in the experiment, such as the dependence of the optical power of the preamplifier on the control current. The

presence of the collapse of the laser emission caused by a thermal mismatch of both DBR sections of the investigated structure, which was previously observed in the experiment, was demonstrated. Numerical simulations show a transition between the operating modes of the MOPA system and a multi-section laser if the reflection coefficient of the front facet increases. For stable MOPA operation, a front facet reflectivity of 10^{-6} or less is required for the proper operation of the system. The theoretical results obtained are in agreement with the available experimental data. (Chap.4, §4.2- §4.6).

4. Numerical calculations demonstrate self-pulsations and short-duration pulses in lasers of various types. The domains of self-pulsations in blue light lasers have been plotted in the plane of different material and geometric laser parameters. The laser structure is grown in the vertical direction, the so-called "sandwich". It was concluded that the thickness of the absorber, as well as the lifetime of the charge carriers in the absorber, play an essential role in the laser dynamics, in particular, in the occurrence of self-pulsations. Self-pulsations with frequencies in the range of 0.55-5.00 GHz have been detected by numerical calculations. (Chap.5, §5.2, §5.3).
5. The results of the investigations of an excitable DFB laser with a built-in passive dispersive reflector demonstrate the generation of short pulses. Within the rate equation model, a set of parameters was first sought when the system operates in the excitable regime. In the excitable regime, a small perturbation was injected into the system and the signal at the laser output was analyzed. In particular, we obtained symmetrically shaped pulses. Increasing the ratio of the charge carrier to the photon lifetime reduces the pulse amplitude. We also injected the perturbation sequence into the system and studied the signal at the laser output. It was found that for small perturbations no laser response is observed. On the other hand, when the perturbation is above the threshold, the periodic response was observed. (Chapter 5, §5.4, §5.6)

Recommendations:

1. Further adjustment of software programs and algorithms for different requirements of experimental investigations in the field of laser physics;
2. Expanding the investigations to include various nonlinearities that were excluded in the first approximation;
3. The laser emission control methods used in the thesis could have various practical applications in other fields such as biology, chemistry, etc.;
4. The use of self-pulsed lasers in medicine appears to be interesting from an application point of view.

BIBLIOGRAPHY

1. DAVID, JK, Introduction to Semiconductor Lasers for Optical Communications. In: An Applied Approach, ISBN 978-3-030-24500-9 ISBN 978-3-030-24501-6 (eBook)<https://doi.org/10.1007/978-3-030-24501-6>
2. YASUHIKO, A., TAKAHIRO, N., JINKWAN, K., Chapter Three - Quantum dot lasers for silicon photonics. In: Semiconductors and Semimetals, Elsevier, 2019, vol. 101, pp. 91-138, ISSN 0080-8784, ISBN 9780128188576, <https://doi.org/10.1016/bs.semsem.2019.07.007>
3. CHRISTIAN, O., Dynamics of Quantum Dot Lasers. ISSN 2190-5053 ISSN 2190-5061 (electronic) ISBN 978-3-319-03785-1 ISBN 978-3-319-03786-8 (eBook). DOI 10.1007/978-3-319-03786-8
4. ASADA, M., MIYAMOTO, Y., SUEMATSU, Y., Gain and the threshold of three-dimensional quantum-box lasers. In: IEEE J. Quantum Electron, 1986, vol. 22, pp. 1915–1921. <https://doi.org/10.1109/JQE.1986.1073149>
5. OTA, Y., Thresholdless quantum dot nanolaser. In: [*Express Option*, 2017, vol. 25, p. 19981.](#)
6. LÜDGE, K., SCHÖLL, E., Quantum-dot lasers-desynchronized nonlinear dynamics of electrons and holes. In: IEEE J. Quantum Electron 45(11), 2009, pp. 1396–1403.
7. BROX, O., BAUER, S., RADZIUNAS, M., WOLFRUM, M., SIEBER, J., KREISSL, J., SARTORIUS, B., WUNSCH, H.-J., High-Frequency Pulsations in DFB- Lasers with Amplified Feedback. In: IEEE J. of Quantum Electronics, 2003, vol. 39, pp. 1381-1387.
8. SCHNEIDER, K., MARCENAC, D., Modeling Self-Pulsating DFB Lasers with Integrated Phase Tuning Section. In: IEEE Journal of Quantum Electronics, 2000, vol. 36, pp. 1026-1034.
9. BANDELOW, U., WUNSCH, H.-J., SARTORIUS, B., Dispersive self Q-switching in DFB-lasers: theory versus experiment. In: IEEE Journal of Selected Topics in Quantum Electronics, 1997, vol. 3, pp. 270-278.
10. Vu, TN, KLEHR, A., SUMPFF, B., WENZEL, H., ERBERT, G., TRÄNKLE, G., Wavelength stabilized ns-MOPA diode laser system with 16 W peak power and a spectral line width below 10 pm Semicond. In: Sci. Technol., 2014, vol. 29, no. 035012.
11. AUST, R., Mode Selection and Tuning Mechanisms in Coupled-Cavity Terahertz Quantum Cascade Lasers. In: Optical and Quantum Electronics. vol. 48. 2016, no. 2, 109.
12. LUEDGE, K., "Nonlinear laser Dynamics - From Quantum Dots to Cryptography", (WILEY-VCH Weinheim, Weinheim, 2012), chap. 1, p. 3-34.

13. TRONCIU, V., WERNER, N., WENZEL, H., WÜNSCHE, H.-J. Feedback sensitivity of detuned DBR semiconductor lasers. In: IEEE J. Quantum Electron. 2021, vol. 57(5), p1.
14. WENZEL, H., SHAMS-ZADEH-AMIRI, R., BIENSTMAN, P., A comparative study of higher order Bragg gratings: Coupled-mode theory versus mode expansion modeling. In: IEEE J. Quantum Electron., vol. 42, no. 1, pp. 64–70, 2005.
15. SIEBER, J., ENGELBORGH K., T. LUZYANINA, G., SAMAEY, ROOSE, D., DDE-biftool manual-Bifurcation analysis of delay differential equations, 2016
<https://arxiv.org/pdf/1406.7144.pdf>.
16. TROPPEZ, U., KREISSL, J., Designs break bandwidth record. In: Nature Photonics, vol. 15, no. 1, pp. 4–5, 2021.
17. ZINK, C., MAAßDORF, A., FRICKE, J., RESSEL, P., MAIWALD, M., SUMPFF, B., ERBERT, G., TRÄNKLE, G., Diffraction limited 1064 nm monolithic DBR-master oscillator power amplifier with more than 7 W output power. In: Proc. SPIE, 2018, 10553, 105531C.
18. RADZIUNAS, M., WÜNSCHE, HJ, Multisection lasers: longitudinal modes and their dynamics. In: Piprek, J. Optoelectron Devices, 2005, pp. 121–150.
19. TRONCIU, VZ, YAMADA, M., TOMOKI, M., SHIGETOSHI, O., TOSHIYUKI, I., MOTOTAKA, K. Self-pulsation in an InGaN laser - theory and experiment. In: IEEE J. Quantum Electronics, 2003, vol. 39, pp. 1509-1514.
20. YAMADA, M., "A theoretical analysis of self-sustained pulsation phenomena in narrowband semiconductor lasers, In: IEEE J. Quantum Electron., 1993, Vol. 29, pp. 1330–1336.
21. TRONCIU, V., WUENSCH, H.-J., SIEBER, J., SCHNEIDER, K., HENNEBERGER, F. Dynamics of single mode semiconductor lasers with passive dispersive reflectors. In: Optics Communications, 2000, vol.182 (1-3), pp. 221-228.
22. TRONCIU, V., WUENSCH, H.-J., SCHNEIDER, K., RADZIUNAS, M. Excitability of laser with integrated dispersive reflector. In: SPIE Proceedings, Physics and Simulation of Optoelectronic Devices IX, 2001, vol.4283.

Annex 1. List of publications on the topic of the thesis

Articles in ISI and SCOPUS-listed international journals:

- [A1] TRONCIU, V., GRIGORIEV, E., ZINK, C., WENZEL, H.. Characteristics of monolithic multisection distributed-Bragg-reflector master-oscillator power-amplifiers. In: Optical and Quantum Electronics, 2022, no. 9 (54), p. 0. ISSN 0306-8919. DOI:

10.1007/s11082-022-03953-9.

Available:<https://link.springer.com/article/10.1007/s11082-022-03953-9> (WoS IF: 2,794)

- [A2] **GRIGORIEV, E.**, RUSU, S., TRONCIU, V., New Characteristics of Blue Self-pulsating InGaN Lasers, 2023 IFMBE Proceedings, September 20-23, 2023, Chisinau. Chisinau: Edition 6, pp. 59, ISBN: 978-9975-72-773-0.<https://link.springer.com/book/10.1007/978-3-031-42775-6>(SCOPUS)
- [A3] **GRIGORIEV, E.**, TRONCIU, V., Investigation of Dynamical Properties of a Laser with Incorporated DBR Section Under the Influence of External Optical Feedback, 2022 IFMBE Proceedings, November 3-5, 2021, Chisinau. Chisinau: Pontos, 2022, Issue 5, pp. 439-447. ISSN 16800737. DOI: 10.1007/978-3-030-92328-0_57. Available:https://link.springer.com/chapter/10.1007/978-3-030-92328-0_57(SCOPUS).
- [A4] **GRIGORIEV, E.**, RUSU, S., TRONCIU, V., Influence of Double Feedback on Stationary States of Quantum Dots Lasers, 2022 IFMBE Proceedings, November 3-5, 2021, Chisinau. Chisinau: Pontos, 2022, Issue 5, pp. 3-10. ISSN 16800737. DOI: 10.1007/978-3-030-92328-0_1. Available:https://link.springer.com/chapter/10.1007/978-3-030-92328-0_1(SCOPUS).

In journals from the National Register of specialized journals, indicating the category:

- [A5] Andronic Silvia, **GRIGORIEV, E.**, TRONCIU, V., Generation of high amplitude pulses with excitable DFB lasers and an integrated dispersive reflector, 2022 Journal of Engineering Sciences, 2022, vol. 29, no. 1, pp. 17-22. ISSN 2587-3474. DOI: 10.52326/jes.utm.2022.29(1).02. Available:https://jes.utm.md/2022/03/19/10-52326-jes-utm-2022-29_1_02/(Category B+).
- [A6] **GRIGORIEV, E.**, TRONCIU, V., WERNER, N., WENZEL, H., The influence of a residual reflectivity at the front facet of a multisection master-oscillator power-amplifier, 2022 Journal of Engineering Sciences, 2022, vol. 29, no. 2, pp. 62-67. ISSN 2587-3474. DOI: 10.52326/jes.utm.2022.29(2).06. Available:<https://jes.utm.md/2022/06/10/10-52326-jes-utm-2022-29-2-06/>(Category B+).
- [A7] RUSU, S., **GRIGORIEV, E.**, TRONCIU, V., Stationary states of the laser with quantum dots active medium with optical feedback, 2020 Journal of Science, Innovation, Culture and Art "Akademos, 2020, no. 2(57), pp. 18-21. ISSN 1857-0461. DOI: 10.5281/zenodo.3989139. Available:<https://zenodo.org/record/3989139> ISSN 1857-0461 E-ISSN 2587 – 3687 <https://doi.org/10.52673/18570461>

Proceedings of national conferences with international participation:

- [A8] **GRIGORIEV, E.**, Investigations of pulse generation in lasers with quantum wells as active medium with saturation absorber, 2022 Technical and scientific conference of students, master's and doctoral students, March 29-31, 2022, Chisinau, Republic of Moldova: Tehnica-UTM, 2022, Vol.1, pp. 39-42. ISBN 978-9975-45-828-3. Available:https://ibn.idsi.md/ro/vizualizare_articol/161483

- [A9] **GRIGORIEV, E.**, Characteristics of DBR mop structures with multiple sections, 2021 Technical and scientific conference of students, master's and doctoral students, March 23-25, 2021, Chisinau, Republic of Moldova: Tehnica-UTM, 2021, Vol.1, pp. 35-37. ISBN 978-9975-45-700-2. Available: https://ibn.idsi.md/ro/vizualizare_articol/133720
- [A10] **GRIGORIEV, E.** Study of stationary states and dynamics of a laser with feedback from external cavities, 2020 Technical and scientific conference of students, master's and doctoral students, April 1-3, 2020, Chisinau, Republic of Moldova: 2020, Vol.1, p. 20. ISBN 978-9975-45-633-3. Available: https://ibn.idsi.md/ro/vizualizare_articol/106115
- [A11] **GRIGORIEV, E.**, Study of nonlinear dynamics of blue-violet InGaN lasers, 2019 Technical-scientific conference of students, master's and doctoral students, March 26-29, 2019, Chisinau, Republic of Moldova: 2019, Vol.1, p. 8. ISBN 978-9975-45-588-6. Available: https://ibn.idsi.md/ro/vizualizare_articol/84254
- [A12] OLOINIC, T., RUSU, S., **GRIGORIEV, E.**, TRONCIU, V., Chaos-based optical communication using quantum dot lasers and optical feedback, 2016 Physics and Modern Technologies, August 25-27, 2016, Chisinau, Republic of Moldova: Technical University of Moldova, 2016, 22nd Edition, pp. 78-83. Available: https://ibn.idsi.md/ro/vizualizare_articol/156675

Theses at scientific forums and international conferences

- [A13] **GRIGORIEV E.**, TRONCIU V. The seventh edition of the International Colloquium 'Physics of Materials' - PM-7, University POLITEHNICA of Bucharest, in collaboration with The Romanian Academy of Scientists on November 10-11, 2022. Available:
- [A14] ANDRONIC, S., **GRIGORIEV, E.**, TRONCIU, V., Generation of Pulses with Excitable DFB Laser with Dispersive reflector, 2021 Electronics, Communications and Computing: IC|ECCO-2021, Ed. 11, October 21-22, 2021, Chişinău, Republic of Moldova: Technical University of Moldova, 2021, Edition 11, p. 35. ISBN 978-9975-45-776-7. Available: https://ibn.idsi.md/ro/vizualizare_articol/154860
- [A15] **GRIGORIEV, Yes.**, RUSU, S., TRONCIU, V., Influence of Double Feedback on Stationary States of Quantum Dots Lasers, 2021 Nanotechnologies and Biomedical Engineering, Ed. 5, November 3-5, 2021, Chişinău: Pontos, 2021, Edition 5, R, p. 60. ISBN 978-9975-72-592-7. Available: https://ibn.idsi.md/ro/vizualizare_articol/142325
- [A16] **GRIGORIEV E.**, TRONCIU, V., Investigation of Dynamical Properties of a Laser with Incorporated DBR Section Under the Influence of External Optical Feedback, 2021 Nanotechnologies and Biomedical Engineering, Ed. 5, November 3-5, 2021, Chisinau: Pontos, 2021, Edition 5, R, p. 97. ISBN 978-9975-72-592-7. Available: https://ibn.idsi.md/ro/vizualizare_articol/142591

ADNOTARE

La teza „**Proprietățile laserelor semiconductoare cu mai multe secțiuni și feedback optic**”, prezentată de Eugeniu Grigoriev pentru conferirea gradului de doctor în științe fizice la specialitatea 131.03 „Fizică statistică și cinetică”. Chișinău, 2025.

Structura tezei include: introducere, 5 capitole, concluzii generale și recomandări. Teza se expune pe 137 pagini, bibliografia care constă din 136 titluri, 3 tabele și 64 figuri. Rezultatele prezentate în teză sunt publicate în 16 lucrări științifice.

Cuvinte cheie: lasere semiconductoare, bifurcații, dinamica complexă, feedback optic, MOPA, lasere DFB și DBR, puncte cuantice.

Domeniul de studiu: Fizica laserelor.

Scopul tezei: dezvoltarea și extinderea studiului teoretic al dinamicii neliniare a laserelor semiconductoare cu multi-secțiuni sub influența feedback-ului optic exterior, precum și prezentarea de noi dispozitive cu diferite topologii și stabilirea criteriilor de utilizare a lor în diferite domenii precum, comunicarea optică, spectroscopie, metrologie cuantică, medicină, etc.

Obiectivele: Ajustarea modelului teoretic al laserului semiconductor cu mediu activ puncte cuantice la acțiunea unui feedback optic provenit de la un rezonator Fabry Perot exterior. Elaborarea teoriei laserelor cu reflectoare Bragg distribuite DBR care permit funcționarea în regimul unui singur mod longitudinal cu o lățime a liniei spectrale îngustă, care se află sub influența feedback-ului optic extern. Elaborarea unui model nou cu parametri geometrici și de material dependenți de lungimea de undă a modului primar. Studiul comportamentului dispozitivelor de putere înaltă cu emisie spectrală în bandă îngustă și difracție spațială limitată, așa numitele amplificatoare de putere cu oscilator master integrat monolitic (MOPA). Determinarea mecanismului influenței pompajului dintr-o secțiune asupra secțiunilor alăturate prin încălzirea termică. Investigarea teoretică a colapsului emisiei dispozitivului MOPA observat experimental. Compararea rezultatelor teoretice cu cele experimentale disponibile. Studiarea dinamicii diferitor tipuri de lasere care generează autopulsații și serii de impulsuri de scurtă durată.

Noutatea și originalitatea științifică a rezultatelor: A fost aplicat un model teoretic pentru structura laserului cu puncte cuantice cu feedback dublu și secțiune aer între rezonatoare. Acest model permite obținerea distribuției stărilor staționare a modurilor cavității exterioare în planul diferitor parametri. S-a elaborat teoria laserelor cu reflectoare DBR în regim de funcționare a unui singur mod longitudinal cu o lățime a liniei spectrale îngustă, având parametrii principali ai laserului dependenți de lungimea de undă a modului primar. A fost studiat teoretic mecanismul influenței pompajului din secțiunea PA asupra secțiunii MO prin încălzirea termică a unui dispozitiv multisețional MOPA. A fost confirmat teoretic colapsul emisiei dispozitivului MOPA observat experimental. S-a studiat comportamentul cu atopulsații și de generare a impulsurilor scurte a diferitor tipuri de lasere. S-a determinat mecanismul de generare a impulsurilor de scurtă durată a unui laser de tip DFB.

Problema științifică soluționată constă în propuneri de noi structuri - laser cu mediu activ gropi și puncte cuantice, cu proprietăți controlabile. În rezultatul simulărilor numerice s-au obținut parametri pentru funcționarea adecvată a sistemelor analizate cu utilizare ulterioară în diferite domenii precum spectroscopie, comunicații, medicină, etc.

Semnificația teoretică și aplicativă: În lucrare sunt elaborate modele adaptate teoretic la noi structuri laser cu puncte cuantice și gropi cuantice cu feedback optic și diverse secțiuni. Aceste modele și rezultate teoretice facilitează realizarea experimentală a dispozitivelor studiate în teză pentru îmbunătățirea caracteristicilor lor.

Implementarea rezultatelor științifice: rezultatele acestei teze au fost cu succes implementate în realizarea proiectului din cadrul Programelor de Stat cu cifrul #20.80009.5007.08.

SUMMARY

to the thesis "Properties of multi-section semiconductor lasers under optical feedback.", presented by Eugeniu Grigoriev for the conferment of the degree of doctor in physical sciences in the specialty 131.03 "Physics of statistics and kinetics". Chisinau, 2025.

Dissertation structure includes: introduction, 5 chapters, general conclusions and recommendations. The thesis is presented on 137 pages, the bibliography which consists of 136 titles, 3 tables and 64 figures, the results presented in the thesis are published in 16 scientific papers.

Keywords: Semiconductor lasers, bifurcations, complex dynamics, optical feedback, MOPA, DFB lasers, DBR lasers.

Fields of study: Physics of lasers.

Aim of the work: The development and expansion of the theoretical study of the nonlinear dynamics of semiconductor lasers with active medium pits and quantum dots, as well as the presentation of new devices with different topologies and the establishment of their fields of use in different fields such as optical communication, spectroscopy, quantum metrology, etc.

The objectives: Adjustment of the theoretical model of the semiconductor laser with active medium quantum dots to the action of an optical feedback originating from an external Fabry Perot resonator. Development of the theory of DBR distributed Bragg reflector lasers that enable operation in the regime of a single longitudinal mode with a narrow spectral linewidth, which is under the influence of external optical feedback. New model having the main parameters dependent on the wavelength of the primary mode. Study of the behavior of high-power devices with narrow-band spectral emission and limited spatial diffraction, the so-called monolithic integrated master oscillator power amplifiers (MOPA). Determination of the mechanism of the influence of pumping from the PA section on the MO section through thermal heating. Theoretical investigation of experimentally observed MOPA device emission collapse. Comparison of theoretical and experimental results. Studying the dynamics of different types of lasers that generate self-pulsations and bursts of short duration pulses.

Novelty and scientific originality: A theoretical model was applied for the structure of the quantum dot laser with double feedback and air section between the resonators. This model allows obtaining the distribution of the stationary states, that is, the modes of the external cavity in the plane of different parameters. The theory of lasers with DBR reflectors in the mode of operation of a single longitudinal mode with a narrow spectral line width was developed, having the main parameters of the laser dependent on the wavelength of the primary mode. The mechanism of the influence of pumping from the PA section on the MO section through thermal heating of a multi-section MOPA device was theoretically studied. It was theoretically confirmed the collapse of the MOPA device emission observed experimentally. The self-pulsation and short pulse generation behavior of different types of lasers was studied. The mechanism of generating short duration pulses of a DFB type laser was determined.

The solved scientific problem: consists in proposals of new laser structures, with active medium both pits and quantum dots, with controllable properties. As a result of the numerical simulations, parameters were obtained for the proper operation of the analyzed systems with use in spectroscopy, optical communication, medicine, etc.

Theoretical significance and practical value of the work: In this work, the models are developed theoretically adapted to new laser structures with quantum dots and quantum pits with optical feedback and various sections. Facilitates the experimental realization of the devices studied in the thesis to improve their characteristics based on the theoretical results obtained in the thesis.

The implementation of the scientific results: the studies presented in this thesis were successfully implemented within the project of State Programs #20.80009.5007.08.

GRIGORIEV EUGENIU

**PROPERTIES OF SEMICONDUCTOR LASERS WITH MULTIPLE SECTIONS AND
OPTICAL FEEDBACK.**

131.03 – STATISTICAL AND KINETIC PHYSICS

Scientific summary of the doctoral thesis in physical

Approved for printing 14.02.25

Offset paper. Offset typing.

Printing sheets 2.25

Paper format 60x84 1/16

Edition 25 copies.

Order No. 24

TUM, MD-2004, Chisinau, 168 Stefan cel Mare Blvd.

“Tehnica - UTM” Editorial Department

MD-2045, Chisinau, 9/9 Student Street

@ UTM --- 2025